Direct Triplet Sensitization of Oligothiophene by Quantum Dot

Zihao Xu, Tao Jin, Yiming Huang, Karimulla Mulla, Francesco A. Evangelista*, Eilaf Egap*, Tianquan Lian*

Table of Contents

Materials and Methods

Synthesis of compound T6

Scheme S1. Synthesis of T6.

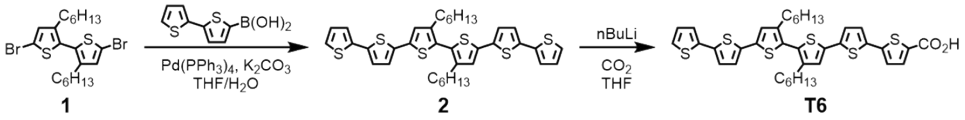

A mixture of compound **1** (428 mg, 0.870 mmol), [2,2'-bithiophen]-5-ylboronic acid[1] (0.402 mg, 1.91 mmol) and $Pd(PPh_3)_4$ (101 mg, 0.0870 mmol) was degassed and backfilled with argon three times before 13 mL THF and 3 mL 2M K_2CO_3 aqueous solution were added by syringe. The reaction mixture was stirred at 70 °C overnight before washed with saturated aqueous NH_4Cl solution and extracted with DCM. The organic layer was dried over anhydrous Na_2SO_4 and purified by column chromatography (SiO_2, 1:20 EtOAc-hexanes) to give the compound **2** as a yellow solid (300 mg, 52%). ^{1}H-NMR (400 MHz, $CDCl_3$): δ = 7.20 (dd, J = 5.1, 1.1 Hz, 2H), 7.16 (dd, J = 3.6, 1.2 Hz, 2H), 7.07 (d, J = 3.8 Hz, 2H), 7.06 (d, J = 3.8 Hz, 2H), 7.04 (s, 1H), 7.02 (dd, J = 5.1, 3.6 Hz, 2H), 2.51 (t, J = 7.9 Hz, 4H), 1.57 (quint, J = 7.0 Hz, 4H), 1.25 (m, 12H), 0.85 (t, J = 7.0 Hz, 6H).

To a solution of compound **2** (320 mg, 0.483 mmol) in 12 mL THF at –78 °C was added *n*-BuLi (0.19 mL, 2.5 M in hexanes) and the mixture was stirred for 3 h. Dry CO_2 was bubbled into the mixture at –78 °C for 1.5 h and at –20 °C for another 1 h during which the reaction turned cloudy. The reaction mixture was stirred overnight at room temperature, poured into 1 M HCl, and extracted with EtOAc. The crude product was purified by column chromatography (SiO_2, 99:1 EtOAc-AcOH) to give the T6 as orange red solid (95.0 mg, 29%). ^{1}H NMR (500 MHz, d_6-DMSO): δ = 13.2 (bs, 1H), 7.65 (d, J = 3.9 Hz, 1H), 7.51 (dd, J = 5.1, 1.1 Hz,1H), 7.43 (d, J = 3.8 Hz, 1H), 7.35 (d, J = 3.8 Hz,1H), 7.31-7.24 (m, 6H), 7.09-7.07 (m, 1H), 2.46 (t, J = 7.3 Hz, 4H), 1.51 (quin, J = 6.2 Hz, 4H), 1.20-1.17 (m, 12H), 0.77 (t, J = 6.6 Hz, 6H); ^{13}C NMR (125 MHz, d_6-DMSO): δ = 163.0, 143.93, 143.89, 142.6, 136.9, 136.5, 136.4, 136.1, 136.0, 135.1, 134.77, 134.74, 133.2, 128.9, 127.4, 127.3, 126.8, 126.7, 126.2, 125.7, 125.5, 125.3, 125.2, 124.7, 31.4, 30.3, 28.9, 22.4, 14.3; ESI-HRMS 706.1195 $[M]^+$; calculated for $[M]^+$ 706.1196.

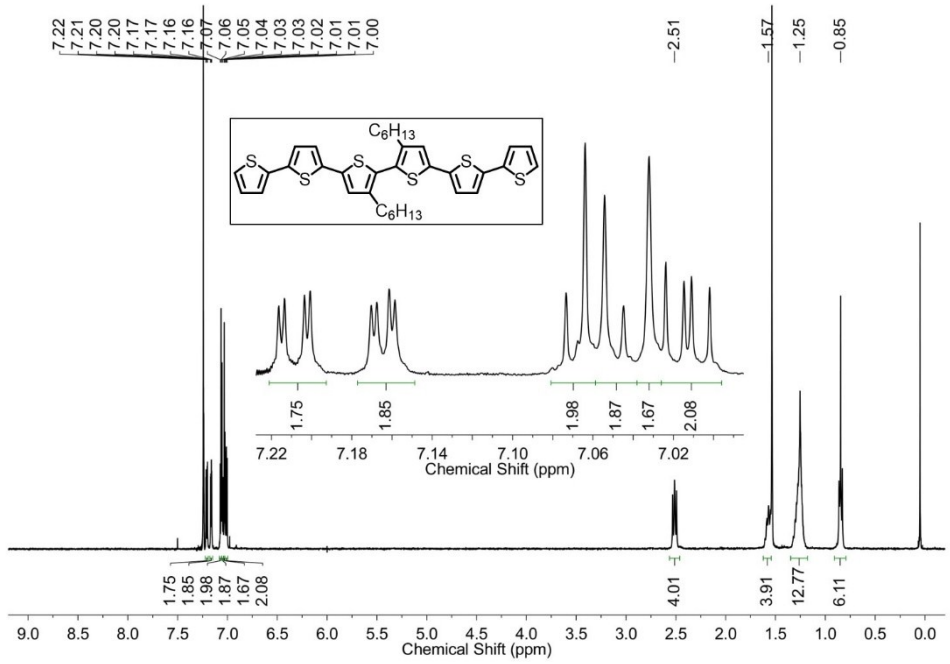

Figure S1. ^{1}H-NMR (400 MHz, $CDCl_3$) spectrum of compound **2**.

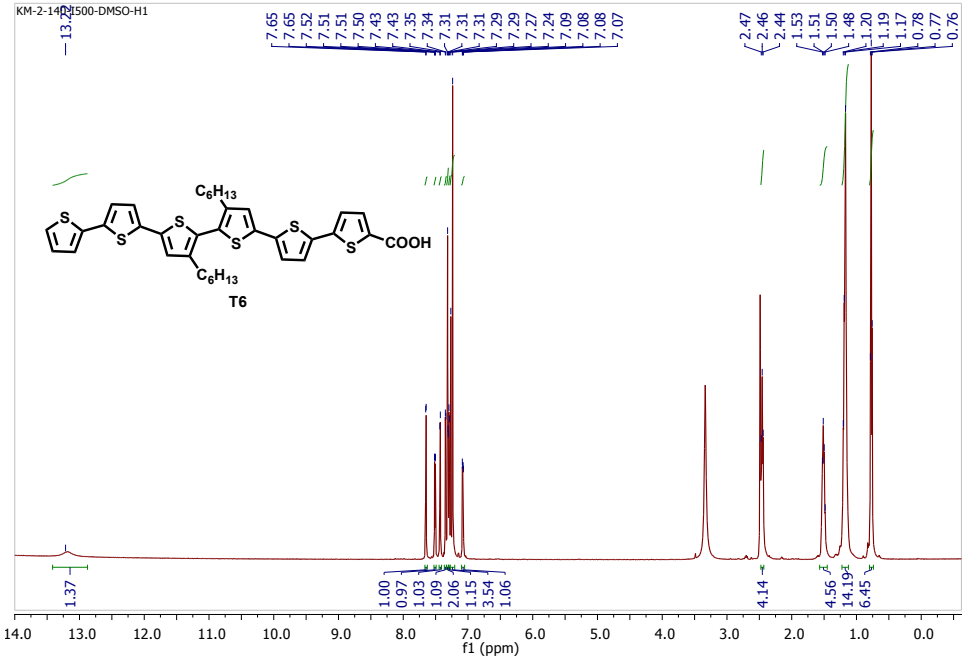

Figure S2. ^{1}H-NMR (500 MHz, $CDCl_3$) of compound T6.

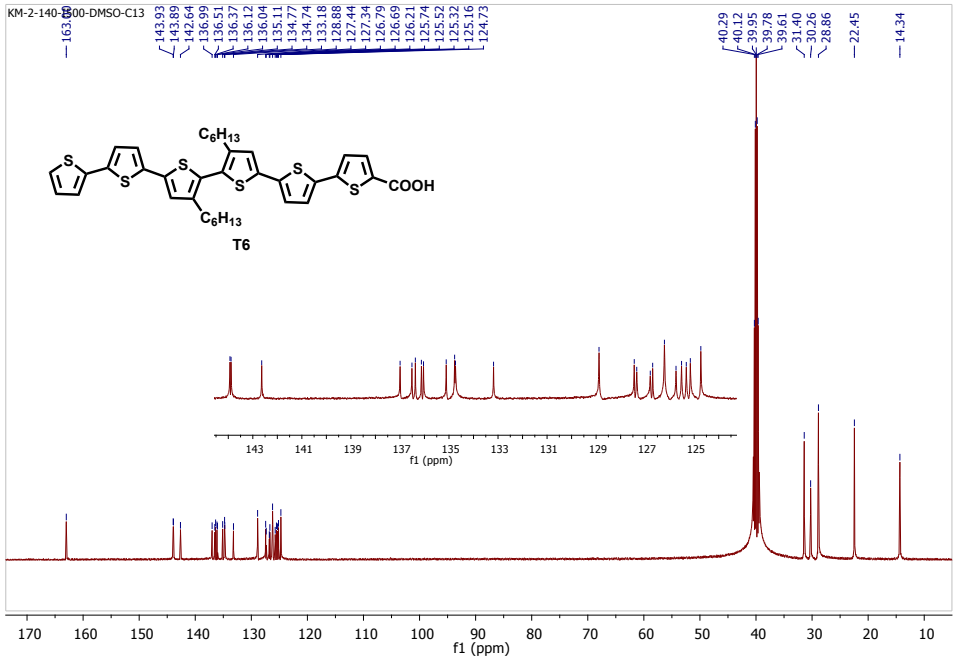

Figure S3. ^{13}C-NMR (500 MHz, $CDCl_3$) of compound T6.

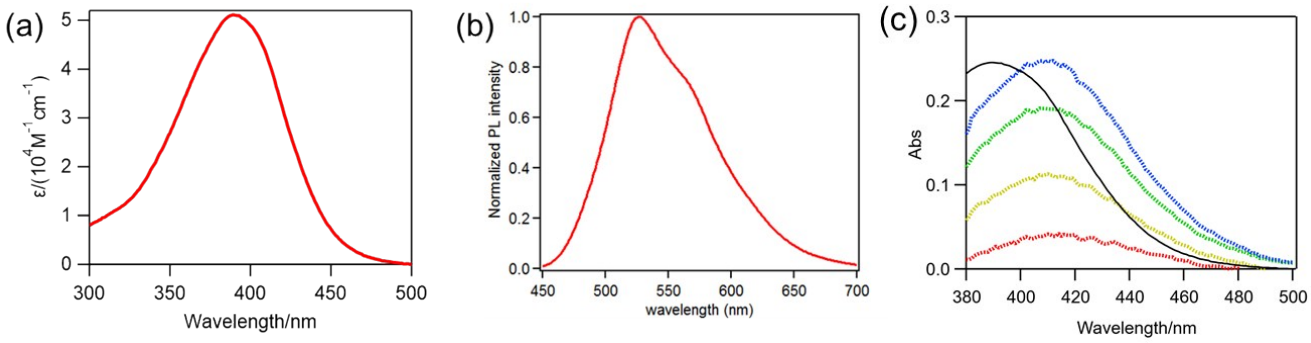

Figure S4. (a) Absorption spectra and (b) steady-state fluorescence of T6 in toluene. (c) Comparison of pristine T6 (black solid line) and QD bounded T6 (dashed line) with increasing T6 concentration (red to blue).

From Fig S4c QD bounded T6 peak maximum shifted from 390 nm to 415 nm, however, based on the concentration of bounded T6, we calculated the peak maximum extinction coefficient at 415 nm to be 4.9×10^5 $M^{-1}cm^{-1}$, very close to the peak maximum extinction coefficient of pristine T6 at 390 nm (5.0×10^5 $M^{-1}cm^{-1}$). This indicates that the dielectric environment didn't change the transition oscillator strength much. In the later text, we used 4.9×10^5 $M^{-1}cm^{-1}$ for GSB extinction coefficient at 415 nm.

The T6 HOMO level was predicted both from theoretical and experimental method to be at -5.49eV.[2] The LUMO was determined to be at -2.31eV by adding the HOMO level and the optical bandgap measured by UV-Vis.

Synthesis of CdSe quantum dot

Cadmium oxide (CdO, 99.5%), selenium powder (Se, 100 mesh, 99.99%), trioctylphosphine oxide (TOPO, 99%), n-octadecylphosphonic acid (ODPA), trioctylphosphine (TOP, 97%) and all other solvents mentioned in synthesis procedures were purchased from Sigma-Aldrich. All chemicals were used without further purification.

CdSe quantum dots were synthesized through a procedure of previous literature[3]. For a typical CdSe synthesis procedure, 120 mg CdO, 560 mg ODPA and 3 g TOPO were mixed in a 50 mL three-neck flask. Upon removing O_2 with Ar, the mixture was heated to 350 °C until the mixture became clear solution. 1 mL TOP was then added into the flask and the system was heated further to 360 °C. After which the solution of 120 mg Se in 1mL TOP was injected quickly into the system. Needle tip aliquots were taken for UV-vis measurement to monitor the reactions until the desired size was achieved. The reaction mixture was then cooled to room temperature, and CdSe was separated by centrifuge and washed twice with toluene and ethanol. The CdSe precipitation was dissolved in toluene. Finally, ligand exchange from TOP to oleic acid was conducted following procedures of previous literature[3]. The CdSe was finally dissolved in toluene and the concentration of CdSe was determined from UV-vis spectrum[4].

The QD VB band edge was determined to be at -5.43eV by the equation[5] $E_{VB} = -5.23 - 0.74D^{-0.95} eV$, the VB band edge is determined to be at -3.31eV by the sum of VB and the band gap obtained from optical transition.

The synthesized T6 powder was dissolved into a toluene solution. 1mL CdSe solution was mixed with certain amount of T6 solution to obtain solutions in which ratios of concentration of CdSe and T6 were 1:1, 2:1, 3:1 and 4:1, respectively. The samples were ultrasonicated for 2 hours at 25 °C and underwent freeze-pump-thaw degassing procedures to remove oxygen in solution. The processed solution was finally stored in a glove box with Argon inert atmosphere and then transferred to a 1 mm path length quartz cell (Starna) for transient absorption experiment.

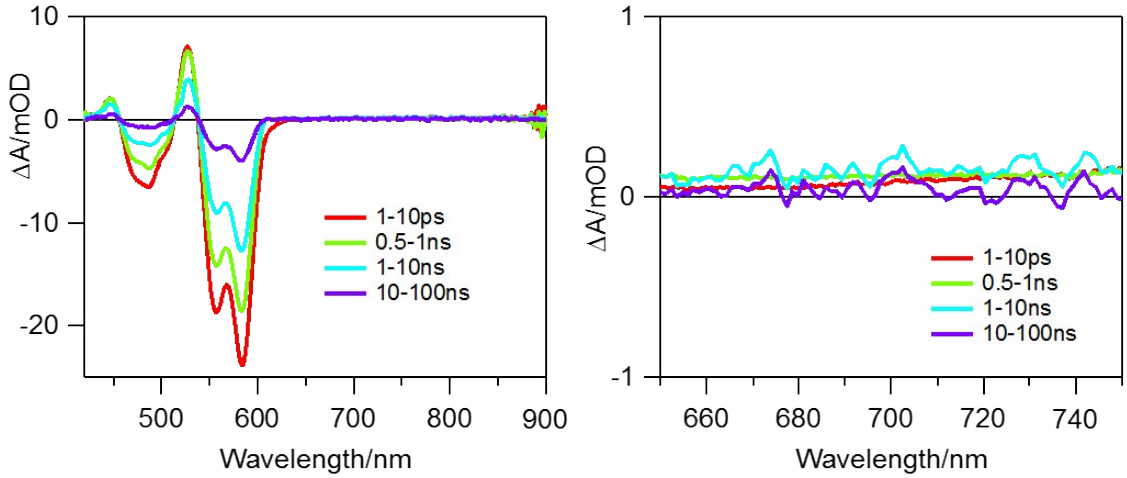

Figure S5. Left: Transient absorption spectrum of 584nm CdSe QD under 520nm excitation. Right: Zoom in region of 650-750nm.

Transient Absorption Spectroscopy Setup

The femtosecond transient absorption is set up based on a regenerative amplified Ti:Sapphire femtosecond laser system (Coherent Legend, 1kHz repetition rate, 150 fs pulse duration and 2 mJ/pulse 800 nm fundamental pulse energy). The data collection used Helios system from Ultrafast Systems, Inc. The fundamental pulse was split in two beams by a 90:10 beam splitter. 10% beam, was focused onto a 2mm sapphire crystal to generate a white light continuum (WLC) probe. WLC was split by a beam splitter to provide the probe for the sample and reference to correct for the fluctuation. The optical fiber to collect the probe is coupled with visible spectrometer and a 1024 elements CMOS camera. For pump beam, such as 520 nm wavelength, 1 mJ of 800 nm fundamental was directed into an optical parametric amplifier (OPA), a signal and an idler NIR pulse are generated. One of the NIR pulse, in 520 nm case the signal, goes through a BBO crystal colinearly with 800 nm pulse, after sum frequency generation (SFG) the desired wavelength is generated. A band pass filter was used to filter out the undesired NIR and 800 nm. A chopper modulated the pump by 500 Hz to block out every other pump to provide absorption signal of excited and un-excited. The pump goes through a delay stage. The diameter of the beam on the sample is 400 μm and 100 μm for pump and probe, respectively. The typical instrument response (IRF) is well fitted by a Gaussian function with 150 fs full width half maximum (FWHM). The chirp was corrected by fitting the solvent response. This setup has the time range of 1.6 nanosecond with a minimal time resolution of ~30 femtosecond.

The nanosecond transient absorption data (beyond 1 nanosecond) is collected using EOS system from Ultrafast Systems, Inc. The pump pulse is the same from femtosecond transient absorption setup. The probe pulse is provided by a low jitter, 0.5 ns pulse duration, 2 kHz, WLC laser (STM-2-UV, Leukos).

The sample is in 1 mm quartz cell (Starna) and constantly stirred during the experiment to avoid photodegradation. All experiments are performed at room temperature.

Steady State Fluorescence setup

Steady state fluorescence was measured with Cary Eclipse fluorometer. The excitation wavelengths were 520 nm for CdSe, CdSe-T6 samples and 390nm for T6 sample.

Supplement results

Determine intersystem crossing rate of T6

To determine the rate of excited state decay processes (singlet and triplet decay and the intersystem crossing rate), kinetics at 415 nm (GSB), 715 nm (singlet+triplet ESA) and 881 nm (singlet ESA) were plotted in Fig S6 and fitted globally with the model described below. From the fitting, the intersystem crossing rate k_{isc} is 0.914±0.008 ns^{-1}, the singlet excited state decay rate k_{SD} is 0.963±0.008 ns^{-1}, and the triplet excited state decay rate k_{TD} is 6.12±0.36×10 ms^{-1}. The similar intersystem crossing rate and singlet decay rate resulted in very high triplet yield at 48.7%. Fitting parameters including extinction coefficients of singlet and triplet excited-states are listed in Table S1.

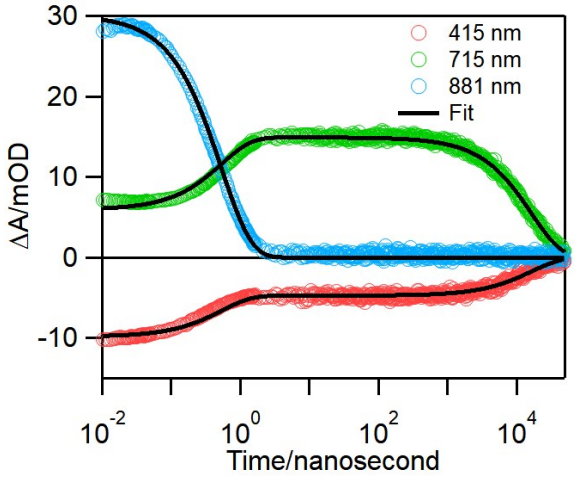

Figure S6. T6 kinetics of ground state at 415 nm, singlet at 881 nm and triplet excited state at 715 nm

Related rate constants could be obtained from fitting of the kinetics at several wavelengths. The singlet excited state ($^{T6}{}^{*}_{S}$) could decay by either intersystem crossing (k_{isc}) or return to the ground state (k_{SD}). The intersystem crossing product, triplet excited state ($^{T6}{}^{*}_{T}$), has only one decay pathway that is another intersystem crossing process to the ground state (k_{TD}). Following this model, it is easy to write the expression for the singlet and triplet excited state kinetics.

$$[T6]^{*}_{S}(t) = [T6]^{*}_{S}(0)e^{-(k_{SD}+k_{isc})t} \qquad \text{Eq S1}$$

$$[T6]^{*}_{T}(t) = \frac{[T6]^{*}_{S}(0)k_{isc}}{k_{SD}+k_{isc}-k_{TD}}[e^{-k_{TD}t} - e^{-(k_{SD}+k_{isc})t}] \qquad \text{Eq S2}$$

Eq. S2 is a solution to Eq. S3 which describes the triplet excited state population growth and decay:

$$\frac{d[T6]^{*}_{T}(t)}{dt} = k_{isc}[T6]^{*}_{S}(t) - k_{TD}[T6]^{*}_{T}(t) \qquad \text{Eq S3}$$

Here, two wavelengths are picked to extract the singlet and triplet excited states. Since there is no available wavelength to represent singlet and triplet population individually, a global fitting is needed. One wavelength is the ground state bleach peak at 415 nm, which the signal kinetics could be written as:

$$\Delta A(415nm) = -\varepsilon_{T6}(415nm)\,[[T6]^{*}_{S}(t) + [T6]^{*}_{T}(t)] \qquad \text{Eq S4}$$

$\varepsilon_{T6}(415nm)$ is the extinction coefficient of ground state at 415 nm obtained from steady state UV-Vis absorbance data. Notice that both singlet and triplet excited state will have a contribution to the ground state bleach. Very importantly, we assumed that the singlet and triplet ESA has very little contribution at 415 nm. The second wavelength is at 715 nm, which is the peak maximum for triplet excited state absorption. This will also serve a purpose to extract the triplet excited state absorption extinction coefficient. However, this wavelength also has a contribution from singlet excited state absorption at early time. Therefore, the expression is written as:

$$\Delta A(715nm) = \varepsilon_S(715nm)[T6]^*_S(t) + \varepsilon_T(715nm)[T6]^*_T(t) \quad \text{Eq S5}$$

$\varepsilon_S(715nm)$ and $\varepsilon_T(715nm)$ is the extinction coefficient of singlet and triplet excited state absorption at 715 nm, respectively. The singlet ESA could be expressed at 881 nm as well by:

$$\Delta A(881nm) = \varepsilon_S(881nm)[T6]^*_S(t) \quad \text{Eq S6}$$

Here Eq. S1 and Eq. S2 is plugged into Eq. S4 to S6, the kinetics could be fitted using these two equations globally. The global fitting curve is shown in Fig S6. The fitting result is in Table S1. In the fitting, the instrument response is also considered and is treated as a convolution with the Eq. S4 and S5. Here, the $\varepsilon_T(715nm)$ is pre-determined by the ratio of the signal amplitude of 715 nm and 415 nm at later time (>10ns) due to complete depletion of singlet excited state at this time range. The fast relaxation from 1ps to 10ps is ignored to simplify the fitting process. The fitting result gave out several critical parameters listed in Table S1 below.

Table S1. Global Fitting parameters of Fig 6.

PARAMETERS	VALUE
$\varepsilon_{T6}(415nm)$	$4.9\times10^4 M^{-1}cm^{-1}$
$\varepsilon_S(881nm)$	$1.14\pm0.006\times10^5 M^{-1}cm^{-1}$
$\varepsilon_S(715nm)$	$2.36\pm0.02\times10^4 M^{-1}cm^{-1}$
$\varepsilon_T(715nm)$	$1.19\pm0.04\times10^5 M^{-1}cm^{-1}$
k_{SD}	$0.963\pm0.008 ns^{-1}$
k_{isc}	$0.914\pm0.008 ns^{-1}$
k_{TD}	$6.12\pm0.36\times10^1 ms^{-1}$
Triplet Yield	48.7±0.8%

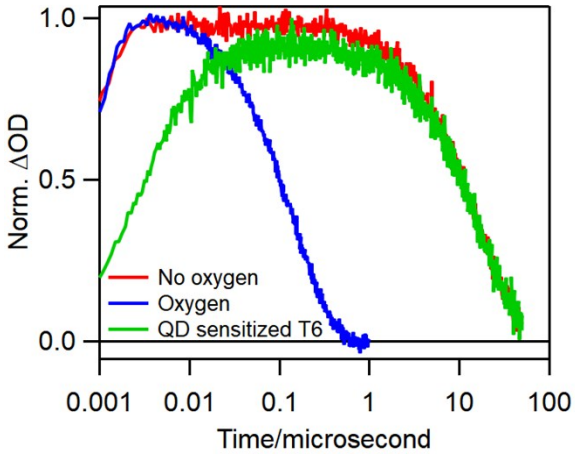

Figure S7. Kinetics of T6 triplet ESA signal at 715 nm: T6 without oxygen (Red), T6 with oxygen (Blue) and CdSe-T6 complex without oxygen (Green) are shown.

In Fig S7 pristine T6 was excited at 400nm. QD-T6 was excited at 520 nm to avoid exciting T6 directly. An exponential fit is used to fit the decay of the T6 triplet excited state decay. The fitting determined the triplet decay rate is $6.12\pm0.36\times10^{1}$ ms^{-1} without oxygen, over 1000 times slower than the energy transfer rate constant, therefore, it is acceptable to fit the growth of triplet excited state population without considering the decay in Fig S6. Comparing the T6 triplet lifetime with and without the presence of oxygen, it is very obvious that the T6 triplet is heavily quenched by ground state triplet oxygen.

Determine the intrinsic TET rate in QD/T6 complexes

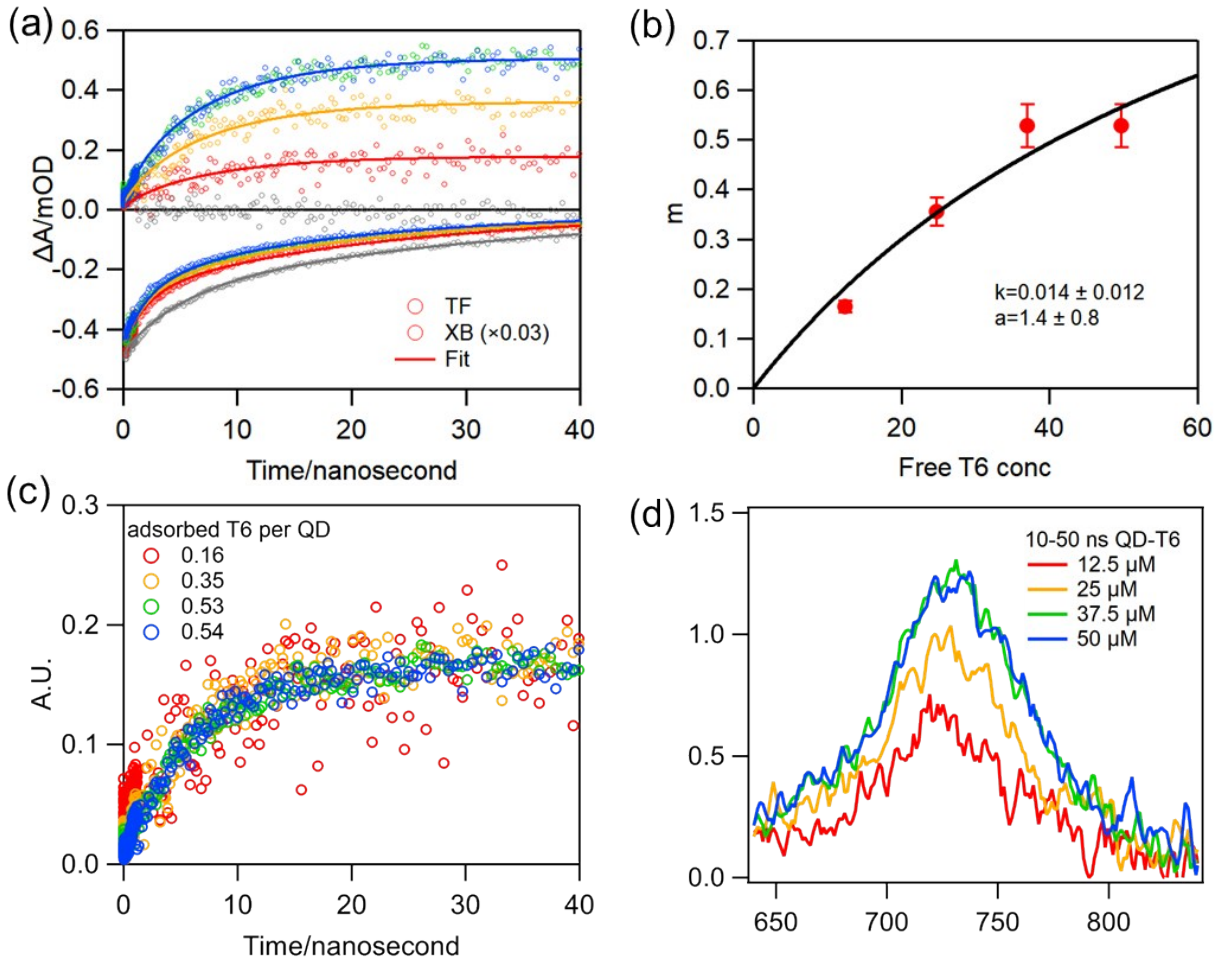

Figure S8. (a) Triplet formation kinetics and QD exciton bleach kinetics (circles, grey: QD only; red, yellow, green, blue: QD+1-4xT6 with increasing loading), global fitting (corresponding color solid line). (b) Average adsorption number of T6 (noted as m) dependence on unbounded T6 concentration (red circle), the black solid line showed the Langmuir isotherm fitting results. Here k is the binding constant, a is the maximum adsorption number. (c) Triplet formation kinetics normalized by the averaged bounded T6 number per QD (m) obtained from the fitting in panel b. (d) T6 triplet signal at maximum amplitude (10-50 ns averaged) TA spectra with increasing T6 concentration.

QD exciton population can be described as:

$$[QD(t)]^* = [QD(0)]^* e^{-(k_1 + ik_{TET})t} \quad \text{(Eq. S7)}$$

During the fitting shown in Fig S8a using Eq. S7, we found that more than one recombination rate k_1 is needed to achieve a reasonable fit. Thus, a coefficient term a_j is added to represent the weight of QD population with different k_{1j}. The apparent triplet energy transfer rate (k_{app}) is obtained from:

$$k_{app} = ik_{TET} \text{ (Eq. S8)}$$

i is the number of T6 attached to each QD surface, k_{ET} is the intrinsic energy transfer rate. The T6 triplet growth kinetics the for QD with i T6 can be written as:

$$\frac{d[T6]_T^*(t)}{dt} = [QD(t)]^* ik_{TET} \text{ (Eq. S9)}$$

Previous studies have shown that adsorption of molecules on QD surface follows a Poisson distribution[6-10]. Considering the probability of finding i T6 on QD where the average number of T6 adsorbed per QD is m, T6 triplet excited state growth is written as below with the consideration of Poisson distribution:

$$[T6]_T^*(t) = [QD(0)]^* \sum_i P(m,i) \sum_j a_j ik_{ET} \left(1 - \frac{e^{-(k_{1j} + ik_{TET})t}}{k_{1j} + ik_{TET}}\right) \text{ (Eq. S10)}$$

To simplify the fitting function, only i=1-4 is considered because all terms where i is larger than 5 are negligible for m<0.5 according to Table S2. Global fitting is used to fit the XB and TF curves in Fig S8a with Eq. S7 and S10 simultaneously. The resulting fitting curves are in solid lines with each curve generating different m value, and the intrinsic TET rate constant being a global parameter is also obtained to be 0.077±0.002ns^{-1}. (m_1=0.16±0.01, m_2=0.35±0.03, m_3=0.53±0.04, m_4=0.54±0.04). The triplet formation kinetics in Fig S8a is scaled based on the m number obtained from the fitting and compared in Fig S8c. The comparison shows similar growth kinetics between different amount of adsorbed T6. This is consistent with the small (<1) m number in these samples. This means that, according to Poisson distribution, the QD has mainly two population. One has no T6 bounded, other has only one T6 bounded. As shown in Table S2, for all T6 concentrations, these two population (0 and 1 T6 per QD) is more than 90% of the total QDs. In conclusion, the efficiency of TET is limited by the adsorbed amount of T6 in this system.

Langmuir isotherm equation is used to obtain the binding constant and maximum adsorption site for QD-T6 complex due to the competitive adsorption[11]:

$$\frac{m}{\theta} = \frac{K[T6]}{1 + K[T6]} \text{ (Eq. S11)}$$

Here θ is the maximum binding sites for T6 per QD, K is the binding constant and [T6] is the concentration of unbound T6. From the UV-Vis spectrum and extinction coefficient, the QD concentration and T6 total concentration (including adsorbed on QD and dissolved in the solvent) can be calculated; the unbound T6 concentration can be calculated as [T6_free] = $[T6]_{total}$-m[QD]. By fitting the data shown in Fig S8b with Eq. S11, the maximum sites and binding constant are obtained. (θ=1.4±0.8, K=0.014±0.012μM^{-1})

The TET efficiency could be estimated by the following equation:

$$\eta = \frac{\Delta A[T6]_T^*}{\varepsilon_T(715nm)} \Big/ \frac{\Delta A[QD]^*}{\varepsilon_{QD}(584nm)}$$

The extinction coefficient of T6 triplet ESA at 715 nm was decided earlier in the pristine T6 fitting, the extinction coefficient of QD is calculated to be $2.238\times10^5 M^{-1}cm^{-1}$ based on previous studies.[3] Notice that the maximum signal amplitude for T6 at 715 nm is 1.6 mOD instead of 0.5 mOD due to the averaging for better signal to noise in the kinetics fitting shown in Figure 4.

Therefore,

$$\eta = \frac{\frac{\Delta A[T6]_T^*}{\varepsilon_T(715nm)}}{\frac{\Delta A[QD]^*}{\varepsilon_{QD}(584nm)}} = \frac{\frac{1.6mOD}{1.19 \pm 0.04 * 10^{-5} M^{-1} cm^{-1}}}{\frac{19.4mOD}{2.24 * 10^{-5} M^{-1} cm^{-1}}} = 15.4 \pm 0.6\%$$

Table S2. Poisson Distribution of P(m, i)

i	0	1	2	3	4	5
P(0.5,i)	0.6065	0.3033	0.0758	0.0126	0.0016	0.0002
P(0.16,i)	0.8521	0.1363	<0.01	-	-	-
P(0.35,i)	0.7047	0.2466	0.0432	<0.01	-	-
P(0.53,i)	0.5886	0.3120	0.0827	<0.01	-	-
P(0.54,i)	0.5828	0.3147	0.0849	<0.01	-	-

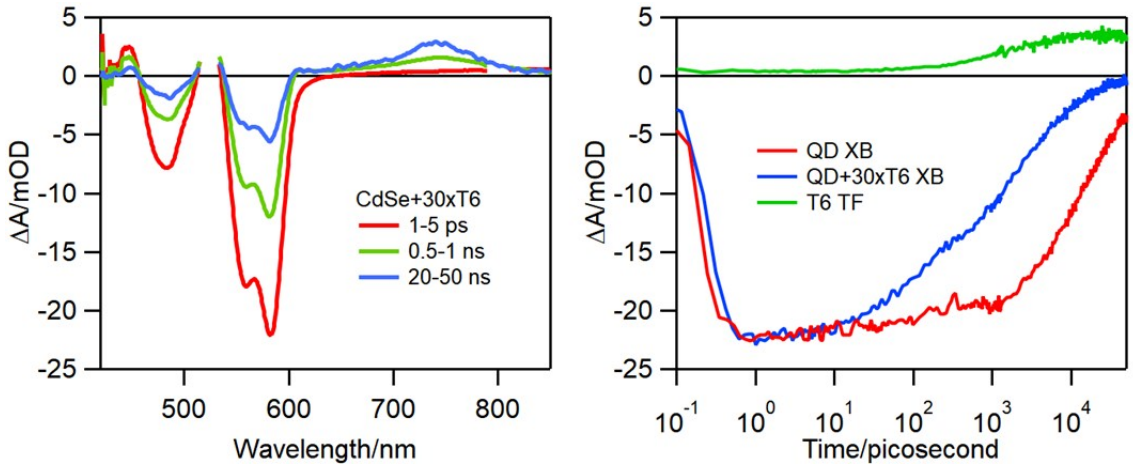

Figure S9. TA spectrum and kinetics at QD XB and T6 triplet ESA of 584 nm CdSe with 30 times concentration (375 μM T6) under 520 nm excitation.

CdSe QD with 375 μM T6 after vigorous sonication could temporarily improve the loading amount of T6 on QD surface, thus improve the overall efficiency. Here it is clearly shown in Fig S9 that the triplet signal of T6 is increased at 20-50 ns TA spectrum. At the same time the QD XB recovery rate is also increased. We could calculate the transfer efficiency as below.

$$\eta = \frac{\frac{\Delta A[T6]_T^*}{\varepsilon_T(715nm)}}{\frac{\Delta A[QD]^*}{\varepsilon_{QD}(584nm)}} = \frac{\frac{3.8mOD}{1.19 \pm 0.04 * 10^{-5} M^{-1} cm^{-1}}}{\frac{22.5mOD}{2.24 * 10^{-5} M^{-1} cm^{-1}}} = 31.8 \pm 1.2\%$$

Theoretical calculation parameters of T6

The DFT equilibrium structure of S_0 deviates from planarity due to a twisting of the C-C bond between the third and fourth thiophene rings by an angle ϕ = 44° (see Fig S10 for the definition of ϕ). Upon excitation to the T_1 state, T6 undergoes a significant rearrangement from a twisted to a planar structure (ϕ = 0°) as shown in Fig S11. The reason for this change in geometry can be traced to the character of the HOMO and LUMO orbitals. While the HOMO is antibonding (π^*) with respect to the middle C-C bond and favors a twisted (ϕ = 90°) configuration, the LUMO is a bonding orbital (π) and favors a planar geometry (ϕ = 0°). Therefore, upon excitation of one electron from the HOMO to the LUMO, it is energetically advantageous for the T_1 state to adopt a planar geometry.

To identify low-lying electronic excited states involved in the triplet-triplet transfer mechanism we performed time-dependent density functional theory (TD-DFT) computations starting from DFT singlet ground state. Vertical excitation energies were performed both at the S_0 and T_1 equilibrium geometries. At the S_0 geometry, T_1 lies 1.85 eV above the ground state and is characterized by a spin-flip HOMO → LUMO excitation. Geometric relaxation of the T_1 state stabilizes it by 0.47 eV, giving an adiabatic S_0 to T_1 transition energy of 1.38 eV. The second triplet state corresponds to a HOMO → LUMO + 1 excitation, with vertical transition energy of 2.10 eV. Interestingly, the energy of the second triplet state does not change significantly upon planarization of the molecule. Inspection of the LUMO + 1 orbital reveals that this orbital does not involve the middle C-C bond, which is likely to reduce the energy dependence with respect to the twisting angle ϕ. The third and fourth triplet states are predicted to lie at higher energies (2.64 and 2.82 eV) and therefore should not be operative in the observed triplet-triplet energy transfer. Configuration interaction singles (CIS) excitation energies for all triplet states are found to be in good agreement (deviation less than 0.2 eV) with those from TD-B3LYP.

Table S3. TD-B3LYP and CIS excitation energies (in eV) for MOLECULENAME computed at the S0 state equilibrium geometry. The geometry was optimized at the restricted B3LYP/def2-SVP level of theory.

	TD-B3LYP	CIS
S_0	0.000	0.000
S_1	2.562	3.459
S_2	2.965	3.992
S_3	3.359	4.837
T_1	1.848	1.747
T_2	2.089	1.904
T_3	2.640	2.480
T_4	2.824	2.774

Table S4. TD-B3LYP and CIS excitation energies (in eV) for MOLECULENAME computed at the T_1 state equilibrium geometry. The geometry was optimized at the unrestricted B3LYP/def2-SVP level of theory. Note that the B3LYP/def2-SVP T_1 state equilibrium geometry, the S_0 state lies 0.349 eV above the ground state equilibrium energy.

	TD-B3LYP	CIS
S_0	0.000	0.000
S_1	2.114	2.337
S_2	2.420	3.545
S_3	2.994	4.360
T_1	1.030	0.719
T_2	1.734	1.520
T_3	2.266	2.061
T_4	2.326	2.638

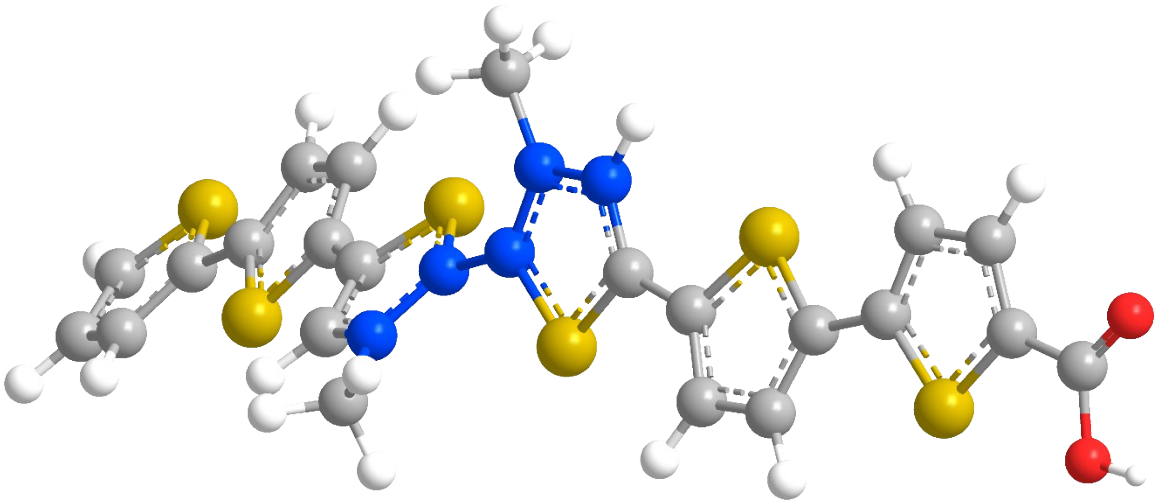

Figure S10. Restricted B3LYP/def2-SVP Equilibrium Geometry of the S_0 state. The twist angle ϕ is defined as the di-hedral angle of the third and fourth thiophene ring as shown in the blue carbon atoms.

Restricted B3LYP/def2-SVP Equilibrium Geometry of the S_0 state (in Å)

C	**-4.169682092254**	**0.729604384336**	**0.126319376121**
C	**-3.971941109583**	**-0.442799914526**	**0.833190826211**
C	**-2.613995827601**	**-0.720288441168**	**1.160350062670**
C	**-1.750893369435**	**0.268025904207**	**0.696010631970**
S	**-2.638399052924**	**1.512165819594**	**-0.168717592383**
C	**-2.205591290004**	**-1.938204100043**	**1.945802342298**
H	**-4.796894685695**	**-1.087288119712**	**1.143706483384**
C	**2.167374710704**	**-0.184117148833**	**0.702136276382**
S	**0.680472447428**	**-1.040014097793**	**0.383920446108**
C	**0.506174874358**	**1.444406253206**	**1.124780601404**
C	**-0.298902638680**	**0.358284096987**	**0.791160413953**
C	**1.891284596038**	**1.120131546687**	**1.071685356642**
C	**0.010108866189**	**2.806937577549**	**1.530108404655**
H	**2.674221519361**	**1.834561896004**	**1.334649159783**
S	**4.934903447054**	**0.084758009123**	**0.576234024631**
C	**3.450301426730**	**-0.841745021917**	**0.574181509622**
C	**3.728826695707**	**-2.192518823755**	**0.431426904635**
S	**8.334193561393**	**-2.649191235181**	**-0.065153257169**
C	**5.111087311091**	**-2.479510976695**	**0.342184531606**
C	**5.918374076465**	**-1.355656959089**	**0.413986450161**
C	**7.362437769654**	**-1.265273752604**	**0.368831866982**
C	**8.168785453680**	**-0.163424509372**	**0.635036384524**
C	**9.807878399024**	**-1.740105421074**	**0.127664796611**
C	**9.548011208823**	**-0.435054145877**	**0.498114730143**
H	**2.950413657889**	**-2.956681892105**	**0.410676075621**
H	**5.512089018142**	**-3.489772483499**	**0.245086022947**
H	**7.766442050081**	**0.805895286590**	**0.932826323749**
H	**10.349378374385**	**0.285254598334**	**0.665263794918**
S	**-10.100239526186**	**2.770420763083**	**-2.200155568322**
C	**-11.599687660259**	**1.931440433055**	**-2.002173618506**
C	**-11.449731619154**	**0.795098727529**	**-1.247363343906**
S	**-6.888472250805**	**0.375715151661**	**-0.364171226683**
C	**-10.109249196236**	**0.596667434061**	**-0.811448416602**
C	**-9.240119730622**	**1.585885617312**	**-1.237897200723**
C	**-7.817549122931**	**1.720648876540**	**-0.991362344230**
C	**-6.996384810534**	**2.817842191921**	**-1.187630691998**
C	**-5.408956383507**	**1.313297688664**	**-0.342684324835**
C	**-5.646249152067**	**2.589588500483**	**-0.825073615865**

H	**-12.507282361552**	**2.325688221579**	**-2.456883501450**
H	**-12.273669220737**	**0.122347809933**	**-1.005040064425**
H	**-9.791290789040**	**-0.240743691797**	**-0.188393422979**
H	**-7.366735665830**	**3.771745099210**	**-1.566538874432**
H	**-4.865553231194**	**3.348680418500**	**-0.895333876557**
H	**12.011330094204**	**-3.913134844560**	**-0.558381119268**
C	**11.141846396412**	**-2.317241714837**	**-0.085278458573**
O	**12.180884766693**	**-1.709645281925**	**0.037097286307**
O	**11.091943552569**	**-3.621439952338**	**-0.439499946537**
H	**-2.986094259975**	**-2.206214795472**	**2.674775695198**
H	**-1.265084450554**	**-1.778904905208**	**2.491602544738**
H	**-2.059691772275**	**-2.813911311438**	**1.289995872080**
H	**0.682296068017**	**3.255322070083**	**2.277994075681**
H	**-1.001375014687**	**2.764822303080**	**1.957464524042**
H	**-0.026361212131**	**3.498070823377**	**0.670516918732**

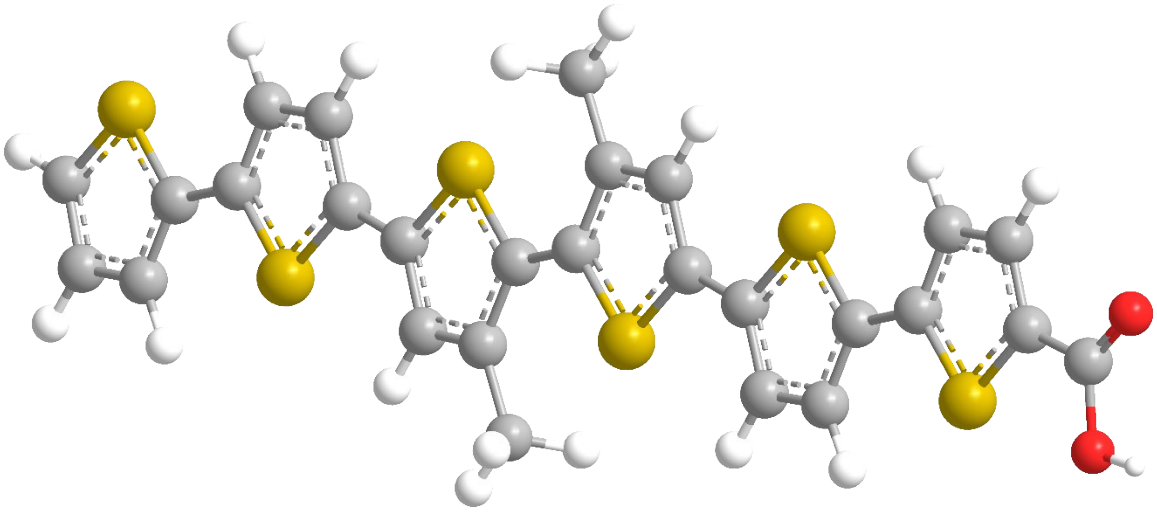

Figure S11. Unrestricted B3LYP/def2-SVP Equilibrium Geometry of the T_1 state.

Unrestricted B3LYP/def2-SVP Equilibrium Geometry of the T_1 state (in Å)

C	**-4.169410339386**	**0.686738621287**	**0.398436276471**
C	**-3.856918780227**	**-0.690818920686**	**0.355155631088**
C	**-2.516031885278**	**-1.004776436176**	**0.229709277424**
C	**-1.663860008439**	**0.171697715333**	**0.165124423415**
S	**-2.689921374201**	**1.632331287507**	**0.274553763766**
C	**-2.039693824928**	**-2.429436352254**	**0.171756116164**
H	**-4.632582607704**	**-1.456647944883**	**0.417764462845**
C	**2.227842052653**	**-0.255401500866**	**-0.200464707669**
S	**0.745224640426**	**-1.204163601911**	**-0.078401299682**
C	**0.575086672289**	**1.439588409737**	**-0.020489126820**
C	**-0.280376289295**	**0.259924462575**	**0.039566442576**
C	**1.909836772307**	**1.131593477302**	**-0.148626703075**
C	**0.093308682645**	**2.861457731629**	**0.047836250130**
H	**2.685658653895**	**1.897275447147**	**-0.207358535830**
S	**4.969243629394**	**0.097880864848**	**-0.450329737342**
C	**3.482945038622**	**-0.857338833585**	**-0.326745141269**
C	**3.800400710159**	**-2.238131169679**	**-0.378311711955**
S	**8.382860436148**	**-2.698429874189**	**-0.819106706146**
C	**5.159563939265**	**-2.499366270672**	**-0.509202112902**
C	**5.966254682172**	**-1.349083105284**	**-0.566022777998**
C	**7.386381061876**	**-1.259771529185**	**-0.696714439232**
C	**8.183471349149**	**-0.109262203521**	**-0.747508530970**
C	**9.837390561293**	**-1.742286102349**	**-0.934864189604**
C	**9.555401529596**	**-0.386429720007**	**-0.880964451345**
H	**3.035418833970**	**-3.013564304353**	**-0.319199340170**
H	**5.577852411850**	**-3.505940399900**	**-0.563844504050**
H	**7.768464702316**	**0.897870107869**	**-0.687903314089**
H	**10.344514920972**	**0.363925379785**	**-0.938969589298**
S	**-10.343336469062**	**3.142657273729**	**0.964444914139**
C	**-11.788641813159**	**2.201109627874**	**1.095705186597**
C	**-11.523187468187**	**0.852960686096**	**1.073167073871**
S	**-6.916532403283**	**0.354982515264**	**0.643457117929**
C	**-10.137559033779**	**0.565994803208**	**0.948822699323**
C	**-9.341945318154**	**1.702626674122**	**0.876417848536**
C	**-7.911525046431**	**1.798752909884**	**0.748026131904**
C	**-7.111307413192**	**2.941246234230**	**0.687066643992**
C	**-5.432490656435**	**1.303240444588**	**0.519208499150**
C	**-5.742113258754**	**2.674667480410**	**0.560934902348**

H	-12.753891275253	2.697880365334	1.182176537546
H	-12.298300001230	0.088429208616	1.143850676335
H	-9.728042455327	-0.444848432104	0.913764561789
H	-7.526583170839	3.949329503416	0.735238043074
H	-4.976782285983	3.449601031615	0.499773152222
H	12.071695583961	-3.972565709719	-1.188459203557
C	11.173863052529	-2.327958773732	-1.071115681255
O	12.200803164539	-1.690805496588	-1.153451519655
O	11.149194714948	-3.681456331385	-1.096665508593
H	-2.896353356007	-3.114620849689	0.246458028152
H	-1.346441130077	-2.667975485464	0.994182969719
H	-1.513364909650	-2.651998322581	-0.770298140430
H	0.947136786782	3.551103353456	-0.015566507928
H	-0.440354867743	3.071277912113	0.988631916888
H	-0.596790318223	3.103079651247	-0.776444756582

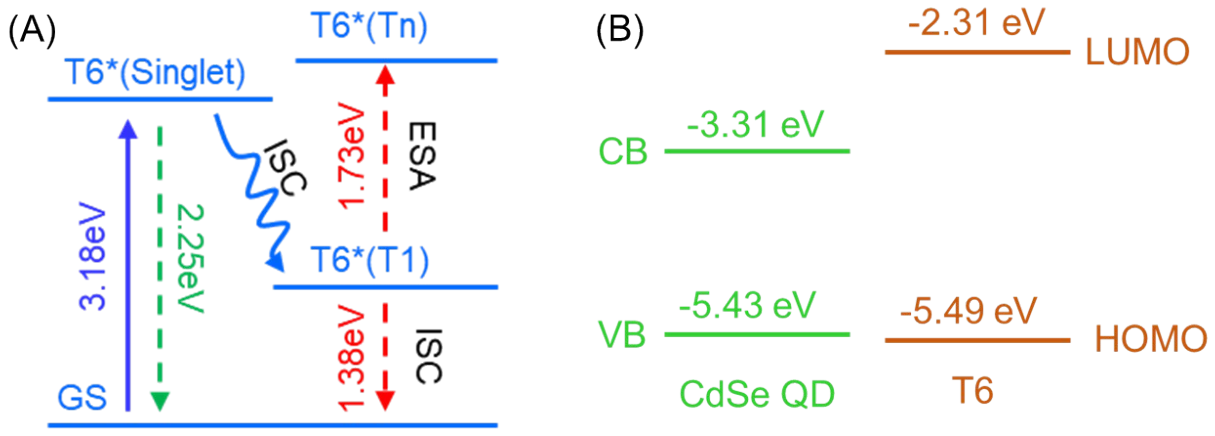

Figure S12. (A) T6 energetics obtained by combination of optical measurements and DFT calculation. The S0 to S1 transition (3.18eV, purple) is measured by UV-Vis absorption. The S1 to S0 emission (2.25 eV, green) is measured by fluorescence spectrum. The T1 excited state energy (1.38eV, red) is obtained by DFT calculation as described above. The T1 to Tn transition (1.73eV, red) is observed by transient absorption measurement. (B) The band alignment between CdSe QD and T6 molecule.

In Figure S12B, the CdSe valence and conduction band edge is calculated from a previous report.[12] The T6 HOMO level is calculated in one of our previous study.[13]

References

1. S. Dufresne, G. S. Hanan and W. G. Skene, *The Journal of Physical Chemistry B*, 2007, **111**, 11407-11418.
2. M. B. Camarada, P. Jaque, F. R. Diaz and M. A. del Valle, *J Polym Sci Pol Phys*, 2011, **49**, 1723-1733.
3. C. Mongin, S. Garakyaraghi, N. Razgoniaeva, M. Zamkov and F. N. Castellano, *Science*, 2016, **351**, 369-372.

4. W. W. Yu, L. Qu, W. Guo and X. Peng, *Chemistry of Materials*, 2003, **15**, 2854-2860.
5. J. Jasieniak, M. Califano and S. E. Watkins, *Acs Nano*, 2011, **5**, 5888-5902.
6. A. Boulesbaa, A. Issac, D. Stockwell, Z. Huang, J. Huang, J. Guo and T. Lian, *J Am Chem Soc*, 2007, **129**, 15132-15133.
7. M. Tagliazucchi, D. B. Tice, C. M. Sweeney, A. J. Morris-Cohen and E. A. Weiss, *ACS Nano*, 2011, **5**, 9907-9917.
8. A. Issac, S. Jin and T. Lian, *J Am Chem Soc*, 2008, **130**, 11280-11281.
9. S. Jin, J. C. Hsiang, H. Zhu, N. Song, R. M. Dickson and T. Lian, *Chem Sci*, 2010, **1**, 519-526.
10. J. Huang, D. Stockwell, Z. Huang, D. L. Mohler and T. Lian, *J Am Chem Soc*, 2008, **130**, 5632-5633.
11. A. J. Morris-Cohen, V. Vasilenko, V. A. Amin, M. G. Reuter and E. A. Weiss, *ACS Nano*, 2012, **6**, 557-565.
12. D. Spittel, J. Poppe, C. Meerbach, C. Ziegler, S. G. Hickey and A. Eychmüller, *ACS Nano*, 2017, **11**, 12174-12184.
13. Y. Huang, Z. Xu, S. Jin, C. Li, K. Warncke, F. A. Evangelista, T. Lian and E. Egap, *Chemistry of Materials*, 2018, **30**, 7840-7851.